



Flexibility of generator and converter

Converter sizing and main circuit component selection for the application



This project has received funding from the European Union's Horizon 2020 research and innovation programme under grant agreement No 764011.

HydroFlex

Increasing the value of hydropower through increased flexibility

Deliverable 4.5 Converter sizing and main circuit component selection for the application

| | |
|--------------------------------|--|
| Work package | WP4 Flexibility of generator and converter |
| Task | Task 4.3 Power electronic interface |
| Lead beneficiary | Chalmers University of Technology (CU) |
| Authors | Chengjun Tang, Torbjörn Thiringer |
| Due date of deliverable | 2021-01-31 |
| Actual Submission date | 2021-01-31 |
| Type of deliverable | Report |
| Dissemination level | Public |

Executive Summary

This report presents the work that was partially done under Task 4.3 of *WP4-Flexibility of generator and converter* and covers entirely the Deliverable 4.5 which aims at choosing the right size and components of the power electronic converter for the application.

The target of the HydroFlex project is to increase the value of hydropower through increased flexibility, and variable speed operation is preferred for achieving that target. One of the important components for the variable speed operation is the power electronic converter, which is the interface between electric machine and grid. The back-to-back configuration of the power electronic converter can decouple the electric machine from the grid side via a DC-link, which means the operation speed of the machine and the reversible turbine is not fixed with the grid frequency (50 Hz) anymore. However, the flexibility of the converter varies with the converter topology, the converter sizing, and the converter components. Therefore, it is valuable to study these factors to investigate the flexibility of the converter. By using a comparative approach, different aspects of the converter are studied and compared in this report, and a conclusion is drawn based on the comparison result.

A major challenge in D4.5 is to simulate the converter performance within a short time and not too much complexity, due to various aspects that need to be studied. To solve the challenge, one method is using the quasi-steady state approach in the simulation, and another method is only considering the grid-side converter in the simulation due to the symmetry of the back-to-back converter configuration. MATLAB Simulink and PLECS are the softwares used in this study to simulate the converter.

It is found through the simulation that the five-level NPC converter with using space vector modulation has the best performance for the studied application, and the Hitachi ABB 6.5 kV power module is the most suitable component for building the converter.

This report contains the following sections:

Section 1 of this report presents the theory of converters. It is composed of three parts: the first part presents the topology of different converters; the second part presents different modulation techniques; the third part presents the methods to quantify the performance of the converter, which are how to calculate the efficiency and current THD of the converter.

Section 2 of this report presents the simulation results concerning different converter topologies and modulation techniques. The converter function check-up is firstly introduced in section 2. Then, the results regarding the converter main component and sizing are introduced.

Section 3 of this report presents the conclusion based on the simulation results in section 2.

Table of Contents

| | |
|--|----|
| Executive Summary | 2 |
| Table of Contents | 3 |
| Abbreviations | 4 |
| 1 Introduction | 5 |
| 2 Theory | 6 |
| 2.1. Converter topologies | 6 |
| 2.1.1 Two-level converter topology | 6 |
| 2.1.2 Neutral-point-clamped converter topology | 6 |
| 2.1.3 Modular multilevel converter topology | 8 |
| 2.2. Modulation techniques | 9 |
| 2.2.1 Pulse width modulation | 9 |
| 2.2.2 Space vector modulation | 9 |
| 3 Converter performance | 10 |
| 3.1 Efficiency | 10 |
| 3.2 Current THD | 11 |
| 4 Simulation results | 12 |
| 4.1 Converter function check-up | 12 |
| 4.1.1 Boundary conditions | 12 |
| 4.1.2 Two-level converter | 12 |
| 4.1.3 Three-level NPC converter | 13 |
| 4.1.4 Five-level NPC, ANPC and MMC converter | 14 |
| 4.2 Converter main component selection | 17 |
| 4.3 Converter sizing | 18 |
| 4.4 Efficiency and current THD comparison | 18 |
| 5 Conclusion | 20 |
| References | 21 |

Abbreviations

| | |
|------|-----------------------------------|
| AC | Alternative current |
| ANPC | Active neutral-point-clamped |
| B2B | Back-to-back |
| CFSM | Converter-fed synchronous machine |
| DC | Direct current |
| DFIM | Double-fed induction machine |
| HVDC | High voltage direct current |
| IGBT | Insulated-gate bipolar transistor |
| MMC | Modular multilevel converter |
| NPC | Neutral-point-clamped |
| PWM | Pulse width modulation |
| SPWM | Sinusoidal pulse width modulation |
| SVM | Space vector modulation |
| THD | Total harmonic distortion |

1 Introduction

With the increase share of the wind and solar energy on the market, the pumped-storage power plants can have a greater role in mitigating the fluctuation brought by these renewable energies in the grid [1]. For pumped-storage hydro power plants, variable speed operation brings more flexibilities over traditional fixed speed operation. It is found that variable speed operation can give a higher overall efficiency for both pumping and turbine mode [2].

To achieve variable speed operation, the power electronic converter is a key interface between the machine side and grid side. Two kinds of configurations have been widely employed in pumped-storage hydro power generation for reaching variable speed operation: the converter-fed synchronous machine (CFSM) and the double-fed induction machine (DFIM). The deciding factor for choosing different configurations here is the rating of the power unit. If the power rating is larger than 100 MW, the DFIM configuration is preferred, while for a rating below 100 MW, the CFSM configuration is more suitable [2]. In this work, a power unit with 65 MW is considered, thus, the CFSM configuration is chosen as the basis of the research. The schematic diagram of the CFSM configuration is shown in Figure 1.

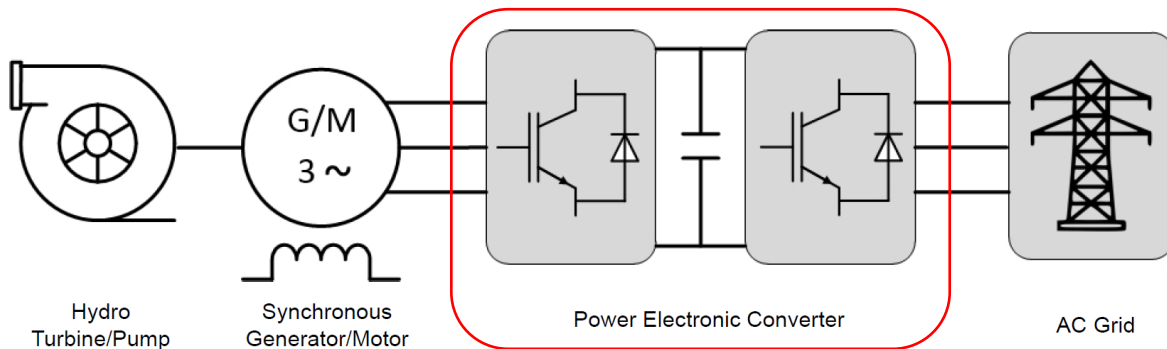


Figure 1 Schematic of a hydro generator connected to the AC grid via a power electronic converter

The power electronic converter, which is marked with a red zone in Figure 1, has the so-called back-to-back (B2B) configuration, which means two converters are connected in series with a DC-link in between them. The presence of the DC-link enables the electric machine to be decoupled from the AC grid, thus, the variable speed operation of the electric machine is achieved. It should be noted that if the output voltage level is not matched with the AC grid voltage level, a transformer is needed to be placed between the converter and the AC grid.

The nominal voltage level of the studied power unit is 13 kV, which is in the medium voltage range. This high voltage level brought challenges to the power switches inside the converter since the maximum blocking voltage of today's semiconductors devices on the market is 6.5 kV [3]. To achieve the voltage and power ratings, a series and parallel connection of power switches are required when building up the converter. In addition to that, the multilevel topology is preferable due to the higher number of voltage levels, lower THD, as well as lower winding insulation stress [1].

2 Theory

2.1. Converter topologies

Power electronic converters have been widely used in different applications, and the main purpose of a power electronic converter in the studied application is to convert AC voltage to DC voltage and vice versa. In this report, the two-level converter topology, the three-level converter topology, and the five-level converter topology are studied and compared.

2.1.1 Two-level converter topology

The two-level converter topology is the most widely used converter topology for various applications. In Figure 2, a simplified circuit diagram of the two-level converter is shown. The two-level converter consists of a DC-link, six groups of active switches and anti-parallel diodes. The IGBT is the type of active switch that studied in this work. As introduced in the theory part, each group of the IGBT and diode pairs consists of several switches and diodes which are connected in parallel and series, due to the lower voltage rating of the switches compared with the converter voltage level.

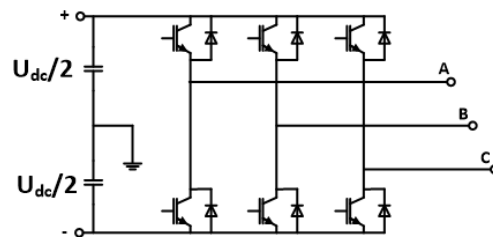


Figure 2 Schematic of a two-level voltage source converter

2.1.2 Neutral-point-clamped converter topology

The neutral-point-clamped (NPC) converter was introduced in [4], and it has been widely used in the high power medium voltage applications [5]. Compared with the traditional two-level converter, the NPC topology can achieve better total harmonic distortion (THD). The 3-level and 5-level NPC topology are shown in Figure 3 and Figure 4 respectively. As can be seen in these figures, clamping diodes and cascaded dc capacitors are employed to produce a multilevel AC voltage waveform. One of the benefits of using the NPC converter is the reduced dv/dt , which means that the stress on the machine winding insulation materials will be decreased compared with two-level converter. Another benefit is the reduced current total harmonic distortion (THD) on the grid side. The NPC converter, especially the three-level NPC converter, has today been practically used in medium voltage applications [6][7].

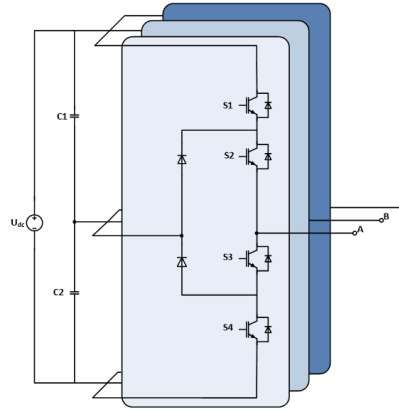


Figure 3 Schematic of a three-level NPC converter

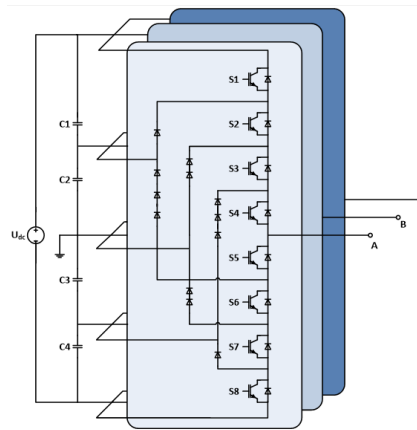


Figure 4 Schematic of a five-level NPC converter

Despite the benefits of the NPC converter topology, it has an issue with the uneven losses among the power switches, which can lead to the unequal junction temperature of the power switches [5]. Therefore, some of the power switches may fail earlier than the others, which could shorten the lifetime of the converter. A solution to this problem is another converter topology, the active neutral-point-clamped (ANPC) converter. By replacing the clamping diodes in the NPC converter with active switch-diode pairs, the uneven thermal stress can be mitigated. In this study, a five-level ANPC converter is studied, and the circuit diagram of it is shown in Figure 5. It can be seen that a flying capacitor C_f is used in the ANPC converter to reach the desired five voltage levels. It should be mentioned that in Figure 5, the voltage over switches S_1 , S_2 , S_3 , and S_4 is half of the DC-link voltage, whereas the voltage over switches S_5 , S_6 , S_7 , and S_8 is a quarter of the DC-link voltage. Therefore, each of the switches S_1 , S_2 , S_3 and S_4 needs two devices in series in the ANPC converter.

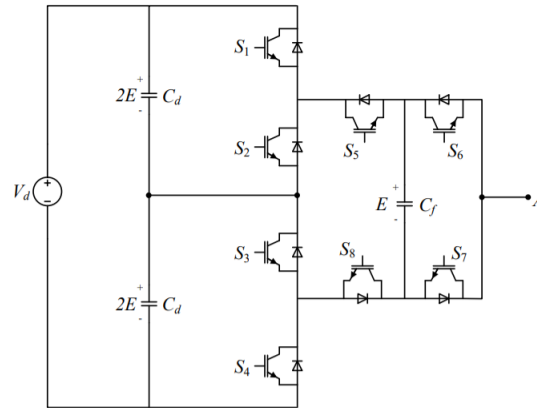


Figure 5 Schematic diagram of one phase of a five-level ANPC converter

2.1.3 Modular multilevel converter topology

The modular multilevel converter (MMC) is being widely used in HVDC transmission applications nowadays. The scalable capability of MMC enables it to achieve higher voltage levels with decreased current THD. An n-level MMC schematic is shown in Figure 6. Compared with the other topologies, arm inductors are needed in the MMC topology, to prevent the in-rush current [5]. The submodules which are denoted as SM in Figure 6 can be the half-bridge submodule, the H-bridge submodule, the flying-capacitor submodule, and the three-level submodule. Among these submodules, the half-bridge submodule has the simplest structure with the least component count. Therefore, in this work, the half-bridge submodule is chosen to be studied.

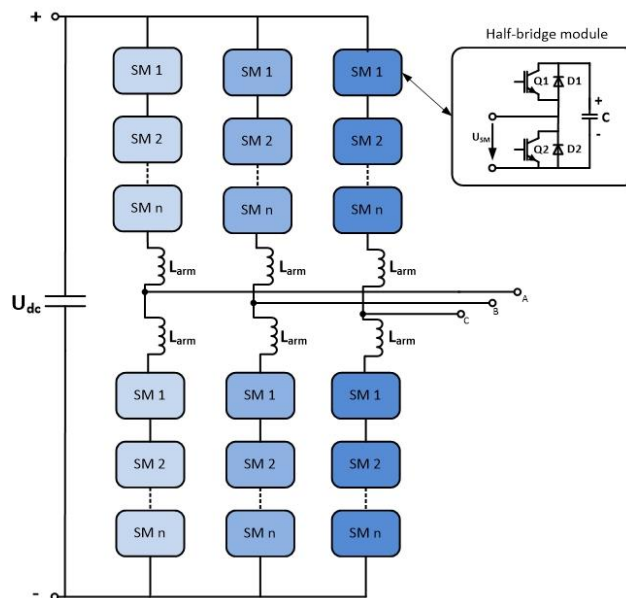


Figure 6 Schematic diagram of the MMC converter

The MMC topology can be extended to electric drives and power generation in medium voltage applications, like for the studied pumped-storage application. The benefits of MMC topology include lower dv/dt , direct fault-tolerant capability, and lower output current THD.

2.2. Modulation techniques

Since the power losses and output waveform quality of the converter are strongly dependant on the modulation techniques, it is important to study the converter topology with various modulation techniques [8]. The modulation techniques are generalized divided into two parts: pulse width modulation and space vector modulation.

2.2.1 Pulse width modulation

Sinusoidal PWM (SPWM) is one of the common modulation techniques to generate the designed output voltage waveforms. Level-shifted PWM and phase-shifted PWM can be used to modulate multilevel converter. Figure 7 shows the modulation of a five-level converter using four level-shifted PWM signals. To maximum utilize the DC link voltage, the third harmonic injection technique can be employed, which is shown in Figure 8. However, the drawback of the SPWM is the difficulty of implication in normal DSP.

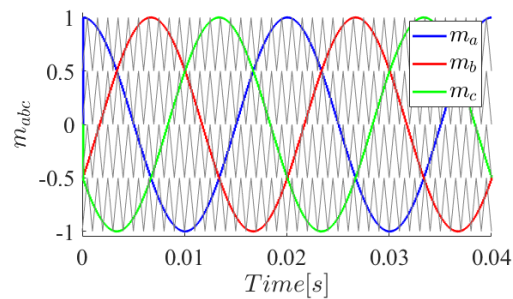


Figure 7 Level-shifted PWM for a 5-level converter

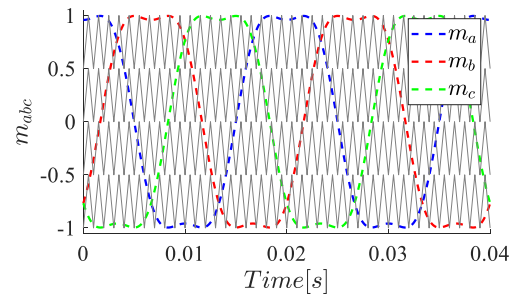


Figure 8 Level-shifted PWM for a five-level converter with third harmonics injection

2.2.2 Space vector modulation

Space vector modulation (SVM) is another commonly used modulation technique. Compared with SPWM, the modulation index of SVM can be 15% higher, which means the DC link voltage can be fully utilized. In other words, a smaller DC link is needed in terms of using SPWM to generate the same output voltage level. However, the complexity of the hexagon diagram increases drastically with respect to the increase of the voltage level. Figure 9 shows the hexagon diagram of a five-level converter. A generalized SVM algorithm is needed when designing the switching sequence of the semiconductors inside the converter. The redundant states of the switches can be used to mitigate the deviation of the neutral point in NPC or to balance the submodule capacitor voltage in MMC.

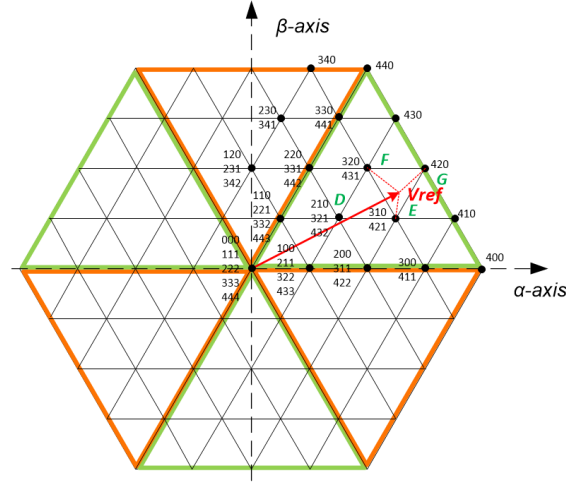


Figure 9 Hexagon diagram of a five-level converter

3 Converter performance

To quantify the performance of the grid-connected converter, efficiency and current THD are the two factors which are used to evaluate it.

3.1 Efficiency

Efficiency is related to the losses of the converter, and in that sense, it determines the lifetime of the converter when the losses affect the semiconductor junction temperature inside the converter. The losses of the converter usually consist of two major parts: the conduction losses P_{con} and the switching losses P_{sw} . Both the two losses are determined by the characteristics of power semiconductors, power ratings, and operation temperature. One way to get the losses is the calculation method [9], which means, based on the data offered by the manufacture, different formulas can be used to calculate the losses.

P_{con} of IGBT and diode can be determined by the following equation respectively,

$$P_{con_IGBT} = \left(\frac{1}{2\pi} + \frac{M \cos(\varphi)}{8} \right) V_{CE0} \hat{I} + \left(\frac{1}{8} + \frac{M \cos(\varphi)}{3\pi} \right) r_{CE} \hat{I}^2$$

$$P_{con_D} = \left(\frac{1}{2\pi} - \frac{M \cos(\varphi)}{8} \right) V_{F0} \hat{I} + \left(\frac{1}{8} + \frac{M \cos(\varphi)}{3\pi} \right) r_F \hat{I}^2$$

where M is the modulation index, $\cos(\varphi)$ is the power factor, V_{CE0} is IGBT forward voltage, V_{F0} is diode forward voltage, r_{CE} is IGBT on resistance, r_F is diode on resistance and \hat{I} is the peak value of output current.

P_{sw} of IGBT and diode can be calculated by

$$P_{sw} = f_{sw} E_{sw} \left(\frac{1}{\pi} \cdot \frac{\hat{I}}{I_{ref}} \right)^{Ki} \cdot \left(\frac{V_{cc}}{V_{ref}} \right)^{Kv}$$

where f_{sw} is the switching frequency, E_{sw} is the loss of each switching action, I_{ref} is the reference current for the calculation, V_{ref} is the referent current for the calculation, V_{cc} is the supply voltage, Ki is the exponent of current dependency and Kv is the exponent of voltage dependency.

Another way of getting the losses is to use a simulation tool, such as PLECS. By inserting a series of data points from the data-sheet to create look-up tables in PLECS thermal model, the losses of an IGBT module can be evaluated. An example of the loss look-up table is shown in Figure 10.

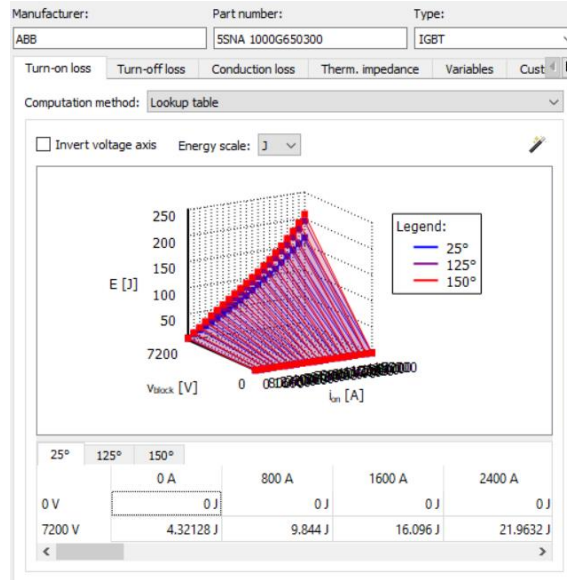


Figure 10 Example of loss look-up table in PLECS

3.2 Current THD

THD is a measurement of the harmonic distortion present in a signal comparing with the fundamental frequency. According to IEEE 519-2014 standard, the limit of grid current THD is 5%. If the current THD is higher than the limit, then a filter is needed. However, the presence of the filter can decrease the overall efficiency of the converter. As introduced in the theory part, the multilevel converter has the benefit of lower THD due to higher voltage levels, thus, it would be interesting to study the current THD of a multilevel converter without the filter. The formula that used to calculate the current THD is,

$$THD = \frac{\sqrt{\sum_{k \neq 1} I_{k,rms}^2}}{I_{1,rms}}$$

4 Simulation results

This part presents the simulation results of different converter topology and modulation techniques. MATLAB Simulink and PLECS are the software used in this study to simulate the converter.

4.1 Converter function check-up

4.1.1 Boundary conditions

To quantify the efficiency of the converter, the used boundary conditions in the simulation are listed as following:

Table 1 Boundary conditions

| | |
|-----------------|--------|
| $V_{LL, rated}$ | 13 kV |
| I_{rated} | 3100 A |
| f_{rated} | 50 Hz |
| $\cos(\varphi)$ | 0.94 |
| V_{dc} | 22 kV |

A three-phase RL circuit is used to represent the load, and the parameters of the RL circuit are listed as following:

Table 2 RL circuit parameters

| | |
|-----|-----------|
| R | 2.276 Ohm |
| L | 0.0026 H |

4.1.2 Two-level converter

In Figure 11 and Figure 12, the phase-to-phase voltage and phase current of a two-level converter are shown respectively. The modulation technique used in the simulation is SPWM, and the switching frequency is $f_{sw} = 1$ kHz. It can be seen that the output current of the two-level converter has a sinusoidal shape, however with relatively high current ripples, which means the current THD is high.

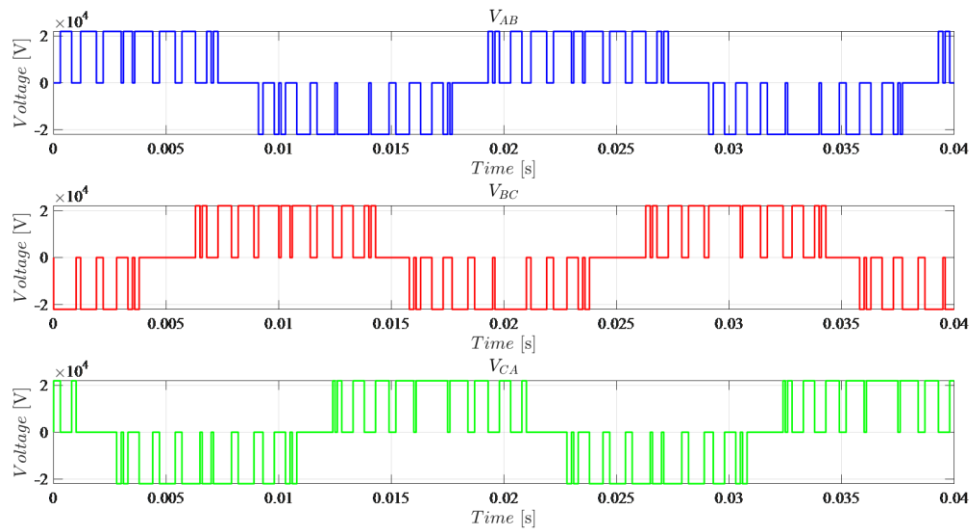


Figure 11 Phase to phase voltage of the two-level converter

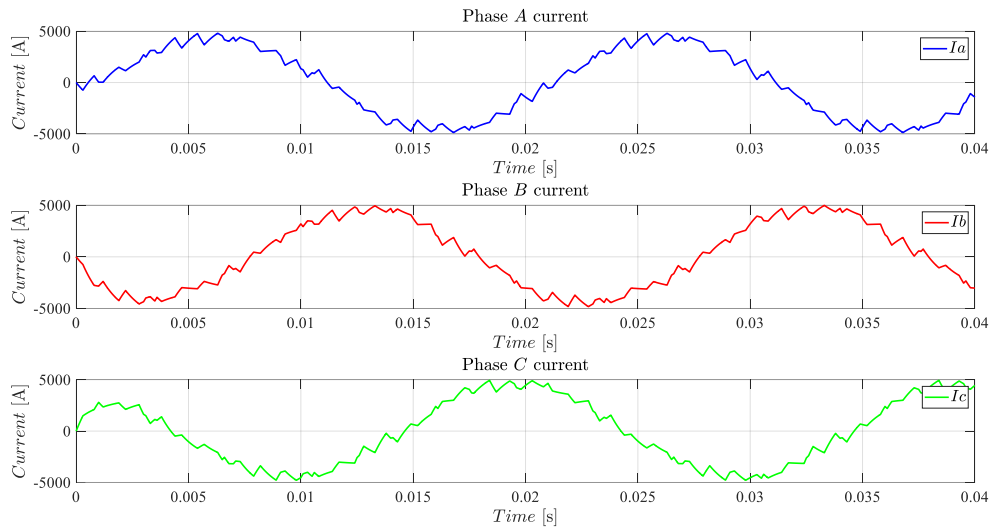


Figure 12 Phase current of the two-level converter

4.1.3 Three-level NPC converter

In Figure 13 and Figure 14, the phase-to-phase voltage and phase current of a three-level NPC converter are shown respectively. The modulation technique used in the simulation is SPWM, and the switching frequency is $f_{sw} = 1$ kHz. It can be seen that the output current of the three-level NPC converter has a more sinusoidal shape compared with the two-level converter.

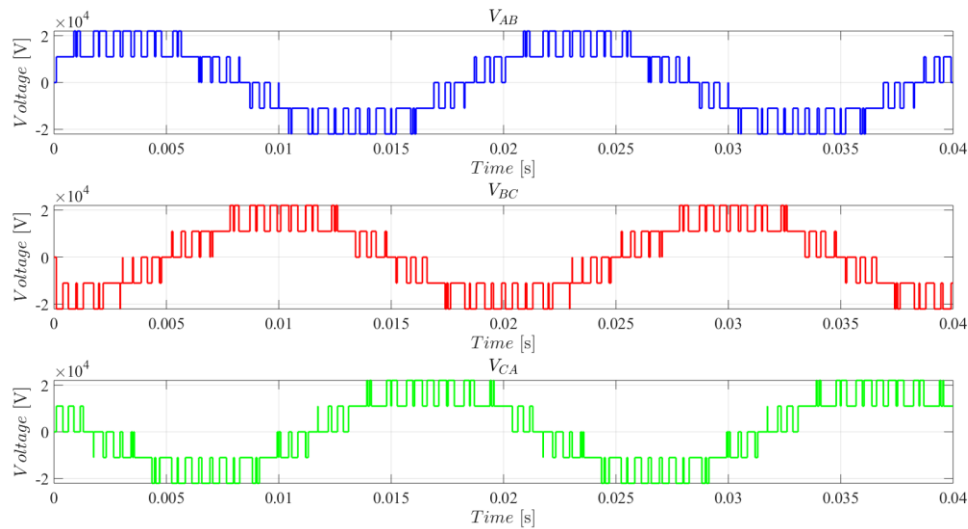


Figure 13 Phase to phase voltage of the three-level NPC converter

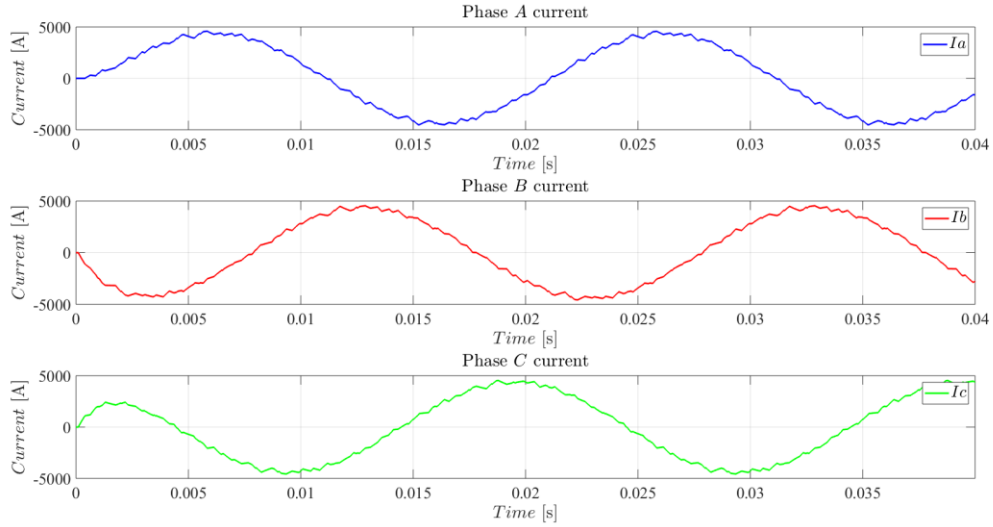


Figure 14 Phase current of the three-level NPC converter

4.1.4 Five-level NPC, ANPC and MMC converter

In Figure 15 and Figure 16, the phase-to-phase voltage and phase current of a five-level NPC converter are shown respectively. The modulation technique used in the simulation is SPWM, and the switching frequency is $f_{sw} = 1$ kHz. It can be seen that the current ripple is greatly decreased due to the high voltage levels.

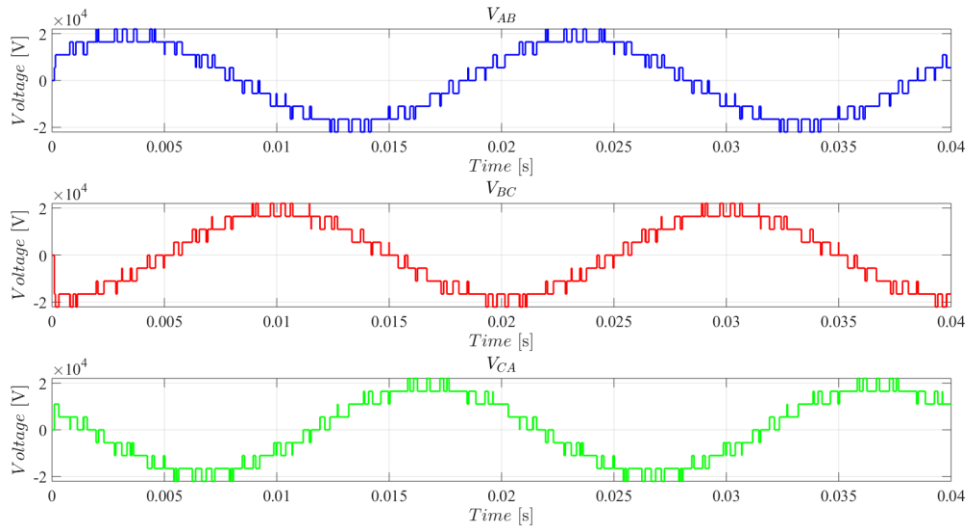


Figure 15 Phase to phase voltage of the five-level NPC converter

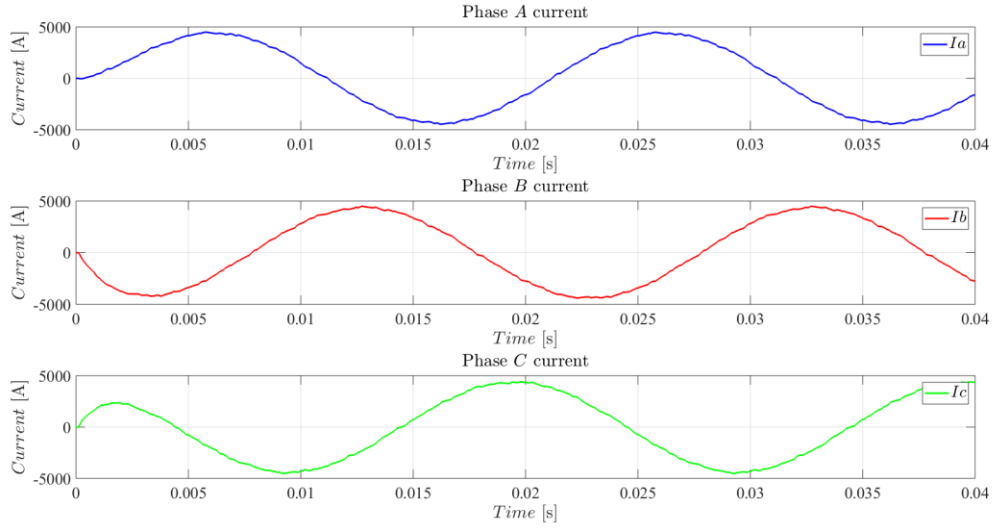


Figure 16 Phase current of the five-level NPC converter

In Figure 17 and Figure 18, the phase-to-phase voltage and phase current of a five-level ANPC converter are shown respectively. The modulation technique used in the simulation is SPWM, and the switching frequency is $f_{sw} = 1$ kHz.

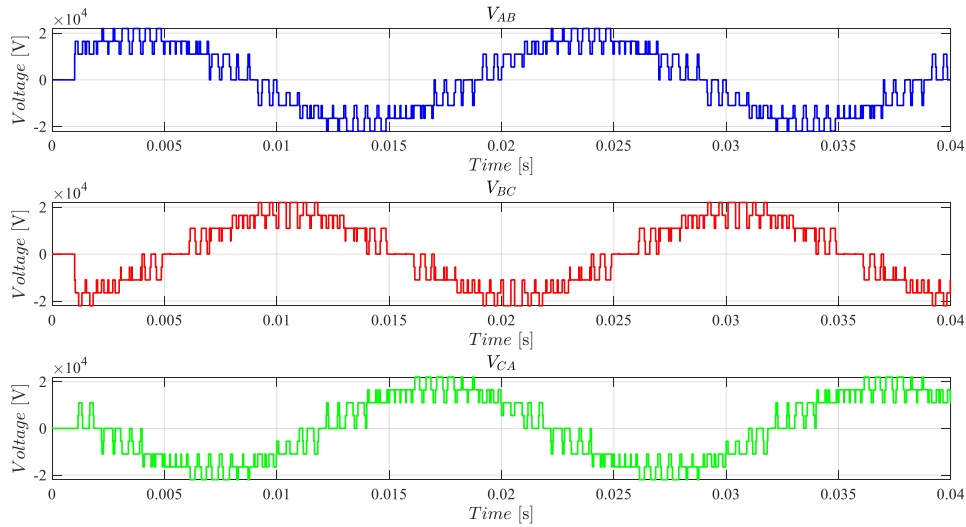


Figure 17 Phase to phase voltage of the five-level ANPC converter

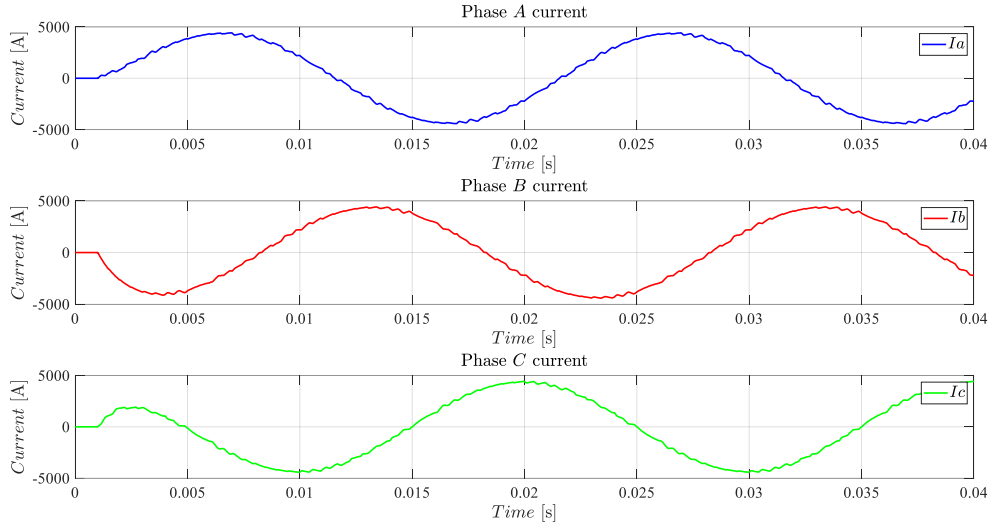


Figure 18 Phase current of the five-level ANPC converter

In Figure 19 and Figure 20, the phase-to-phase voltage and phase current of a five-level MMC are shown respectively. The modulation technique used in the simulation is SPWM, and the switching frequency is $f_{sw} = 1$ kHz.

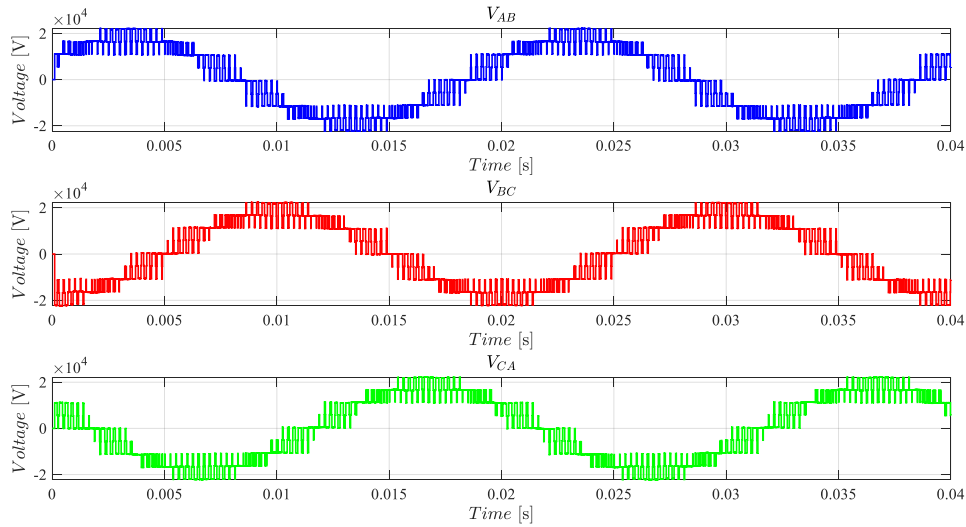


Figure 19 Phase to phase voltage of the five-level MMC

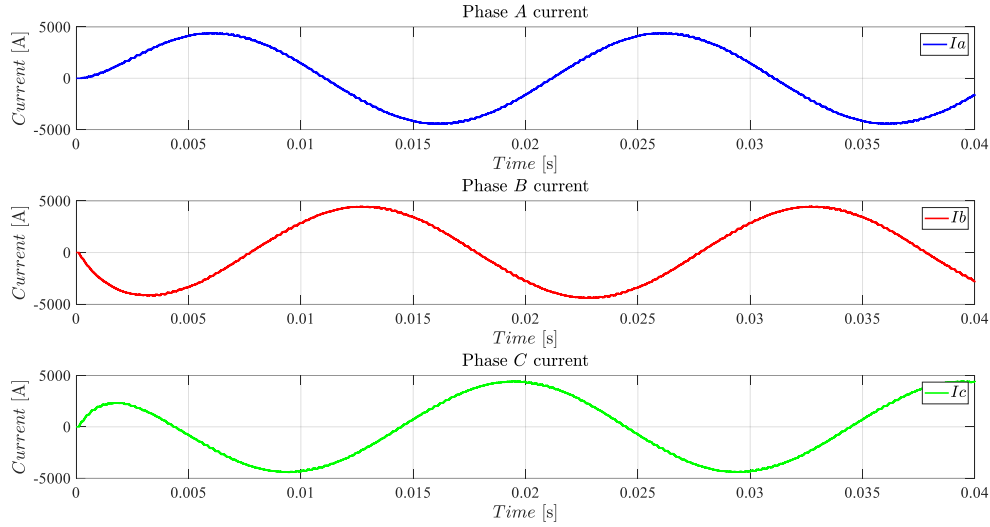


Figure 20 Phase current of the five-level MMC

4.2 Converter main component selection

Component selection is an important part for designing the converter since it determines the converter sizing and efficiency. Due to the constraints of high power and medium voltage for the studied application, the Hitachi ABB high-power IGBT and diode module family are chosen as the basis for selecting the main components. The voltage levels of this power module family are 1.7 kV, 3.3 kV, 4.5 kV, and 6.5 kV voltage.

The priority for selecting the main component is the loss of the power module. As discussed in the theory part, the loss of the power module can be divided into two parts: the conduction loss and switching loss. The conduction loss is related to the IGBT on-state voltage and diode forward voltage. The switching loss is related to the IGBT switching energy and diode reverse recovery energy. The details of the power module family are listed in the following table.

Table 3 Details of the Hitachi ABB high-power IGBT and diode modules

| Part number | V_{ce} (V) | I_c (A) | IGBT V_{on} (V) | V_{on}/V_{ce} | IGBT E_{on} (mJ) | IGBT E_{off} (mJ) | Diode V_f (V) | V_f/V_{ce} | Diode E_{rr} (mJ) |
|------------------|--------------|-----------|-------------------|-----------------|--------------------|---------------------|-----------------|--------------|---------------------|
| 5SNA 3600E170300 | 1700 | 3600 | 3.1 | 1.8e-3 | 1200 | 1690 | 1.9 | 1.1e-3 | 1260 |
| 5SNA 1800G330400 | 3300 | 1800 | 2.9 | 8.8e-4 | 4550 | 4350 | 2.15 | 6.5e-4 | 2250 |
| 5SNA 1500G450350 | 4500 | 1500 | 3.8 | 8.4e-4 | 5860 | 5900 | 2.75 | 6.1e-4 | 5350 |
| 5SNA 1000G650300 | 6500 | 1000 | 4.4 | 6.7e-4 | 5800 | 5650 | 3.35 | 5.1e-4 | 4900 |

It can be seen from the above table that the IGBT on-state voltage and diode forward voltage increases with the voltage rating of the power module, but it does not mean the conduction loss is increased with the voltage rating. To quantify the conduction loss of each module in the same scale, the power rating needs to be considered as well. The ratio of the on-state voltage and voltage rating could be use as an index to compare the conduction loss of the power module. As shown in the above table, the ratio decreases with

the increase of the voltage ratings, which means the conduction loss of the power module would be the least if the 6.5 kV power module is chosen for the same application.

For the switching loss part, it would be difficult to tell which power module is the best directly from the table. However, since the switching frequency for these high-power modules cannot be quite high, then, the conduction loss would be the dominant part of the total losses. In other words, the 6.5 kV module suits the application best in terms of the power loss.

Apart from the above consideration, another benefit of choosing this 6.5 kV power module is the decreased number of the series-connected power modules, which can lead to fewer component counting compared with the other voltage rating power modules.

In general, the selected power module for this application is Hitachi ABB 5SNA1000G650300, which has the 6.5 kV voltage blocking capability and 1000 A DC forward current carrying capability [10].

4.3 Converter sizing

The nominal phase to phase voltage level in this work is 13 kV, and the nominal phase current is 3100 A. From the previous part it is already know that the single commercial power switch cannot handle such high nominal voltage and current level, thus, several power switches are connected in series and parallel to formulate the power switch group.

Apart from the boundary conditions, the main component is selected as the 6.5 kV power module, and the converter sizing is determined by the counting of the components inside the converter, which is shown as in the following table.

Table 4 Component counting of different converter topologies

| | Two-level converter | Three-level NPC converter | Five-level NPC converter | Five-level ANPC converter | Five-level MMC |
|-----------------------------|---------------------|---------------------------|--------------------------|---------------------------|----------------|
| Number of IGBTs | 288 | 288 | 384 | 576 | 384 |
| Number of diodes | 288 | 432 | 960 | 576 | 384 |
| Number of flying capacitors | 0 | 0 | 0 | 3 | 24 |

It can be seen that for the same boundary conditions, the two-level converter needs the least number of components. While for multilevel converters, generally, the number of components increases with the voltage level: the five-level NPC converter needs extra clamping diodes; the five-level ANPC converter needs more IGBTs and diodes, and also extra flying capacitors; the five-level MMC needs fewer number of power switches and diodes whereas extra flying capacitors are needed in the half-bridge submodules.

4.4 Efficiency and current THD comparison

The results of the efficiency and current THD comparison of different converter topologies and switching frequency are shown in the following table, and in Figure 21 the results are visualized.

Table 5 Efficiency and current THD comparison of different converter topologies and switching frequency

| Topology | | Two-level | | Three-level NPC | | Five-level NPC | | Five-level ANPC | Five-level MMC |
|----------|------|-----------|--------|-----------------|-------|----------------|-------|-----------------|----------------|
| | | SPWM | SVM | SPWM | SVM | SPWM | SVM | SPWM | SVM |
| 450 | loss | 0.63% | 0.53% | 0.36% | 0.37% | 0.32% | 0.36% | 0.42% | 0.50% |
| | THD | 15.98% | 14.17% | 8.64% | 5.18% | 3.91% | 4.50% | 6.80% | 4.50% |
| 750 | loss | 0.79% | 0.79% | 0.54% | 0.50% | 0.41% | 0.46% | 0.54% | 0.57% |
| | THD | 9.50% | 8.16% | 4.95% | 4.49% | 2.72% | 2.30% | 3% | 2.24% |
| 1050 | loss | 1.05% | 1.05% | 0.66% | 0.68% | 0.50% | 0.50% | 0.67% | 0.64% |
| | THD | 6.76% | 5.77% | 3.36% | 2.92% | 1.58% | 1.87% | 1.90% | 1.87% |
| 3000 | loss | 2.92% | 2.89% | 1.59% | 1.57% | 0.92% | 0.96% | 1.54% | 1.31% |
| | THD | 2.36% | 1.98% | 1.13% | 1.11% | 0.47% | 0.43% | 0.57% | 0.72% |

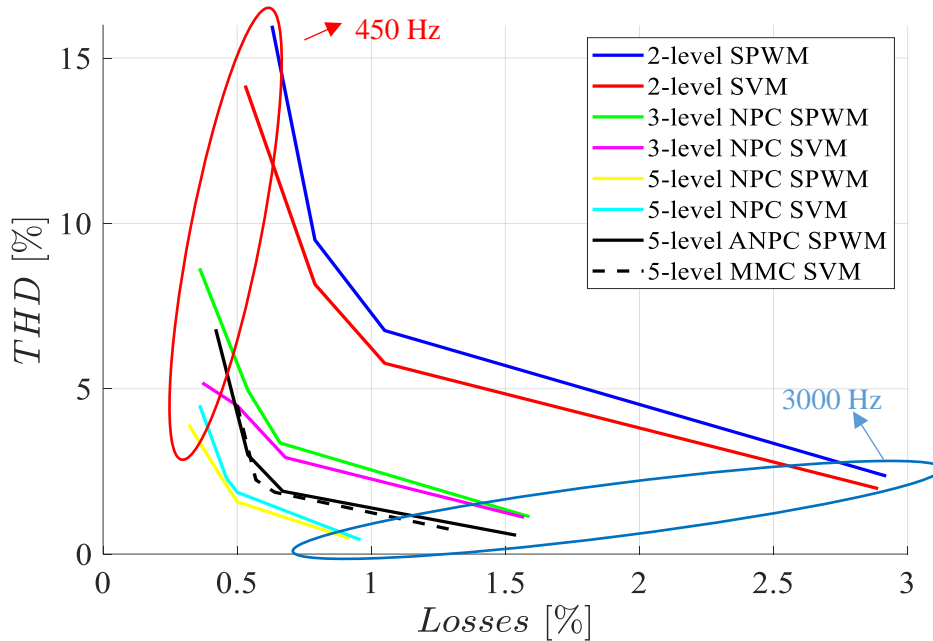


Figure 21 Losses and current THD for different converters with a various switching frequency

In general, Figure 21 shows that:

- 1) SVM can have better results over SPWM due to the higher DC link utilization.
- 2) When the switching frequency increases, the loss increases while the current THD decreases.
- 3) The five-level NPC converter using SVM with 750 Hz switching frequency has the best overall performance regarding the efficiency and current THD. However, the uneven distribution of losses among switches can bring an early failure of the converter. Therefore, tailored cooling method needs to be developed for the five-level NPC converter to mitigate the uneven loss distribution.
- 4) In addition to the five-level NPC, the five-level ANPC converter and the five-level MMC can be alternative converter topologies for the studied application.

5 Conclusion

The present report documents the work that is done to fulfil the Deliverable 4.5, which is about the converter sizing and main component selection. Efficiency and current THD are the two factors that are considered when choosing the most suitable converter topology.

By using a comparative approach to simulate different converter topologies, modulation techniques, and switching frequency, it is shown that the five-level NPC converter has the best overall performance for the application. However, the drawback of uneven loss distribution in the NPC converter can shorten the lifetime of the converter, therefore, tailored cooling strategy should be developed when employing the five-level NPC topology. The five-level ANPC and MMC can be the alternative topologies for the studied high power medium voltage application. In addition to that, the Hitachi ABB 6.5 kV IGBT power module is selected as the main component for designing the converter.

References

- [1] Valavi, Mostafa, and Arne Nysveen. "Variable-Speed Operation of Hydropower Plants: A look at the past, present, and future." *IEEE Industry Applications Magazine* 24, no. 5 (2018): 18-27.
- [2] Holzer, Thomas, and Annette Muetze. "Full-size converter operation of hydro power generators: a state-of-the-art review of motivations, solutions, and design implications." *e & i Elektrotechnik und Informationstechnik* 136, no. 2 (2019): 209-215.
- [3] Du, Sixing, Apparao Dekka, Bin Wu, and Navid Zargari. *Modular multilevel converters: analysis, control, and applications*. John Wiley & Sons, 2017.
- [4] Nabae, Akira, Isao Takahashi, and Hirofumi Akagi. "A new neutral-point-clamped PWM inverter." *IEEE Transactions on industry applications* 5 (1981): 518-523.
- [5] Wu, Bin, and Mehdi Narimani. *High-power converters and AC drives*. John Wiley & Sons, 2017.
- [6] Lee, Kevin, and Geraldo Nojima. "Quantitative power quality and characteristic analysis of multilevel pulsewidth-modulation methods for three-level neutral-point-clamped medium-voltage industrial drives." *IEEE Transactions on Industry Applications* 48, no. 4 (2012): 1364-1373.
- [7] Steimer, Peter K., Osman Senturk, Steve Aubert, and Stefan Linder. "Converter-fed synchronous machine for pumped hydro storage plants." In *2014 IEEE Energy Conversion Congress and Exposition (ECCE)*, pp. 4561-4567. IEEE, 2014.
- [8] Leon, Jose I., Sergio Vazquez, and Leopoldo G. Franquelo. "Multilevel converters: Control and modulation techniques for their operation and industrial applications." *Proceedings of the IEEE* 105, no. 11 (2017): 2066-2081.
- [9] Nicolai, Ulrich, and A. Wintrich. "Determining switching losses of SEMIKRON IGBT modules." *SEMIKRON Application Note, AN 1403* (2014).
- [10] 5SNA 1000G650300, HiPak IGBT module, ABB IGBT Datasheet 5SYA 1465-03, 10-2020